Micro-Texturing for Micro-part based on 2D Image

Gandjar Kiswanto[1,*], Achmad Handryanto[1], Riandhika Hendrianto[1], Ario S. Baskoro[1], D.L. Zariatin[1], Aida Mahmudah[1]

[1]Laboratory of Manufacturing Technology and Automation, Department of Mechanical Engineering,

Universitas Indonesia, Indonesia

[*] gandjar_kiswanto@eng.ui.ac.id

Abstract

Micro-texturing is a process used to produce micro scale texture (pattern) on part surface. Micro-texture is found in many functions, such as for producing tribological performance on a part surface, or giving aesthetic value to product. This paper presents a developed method to produce 3D micro-texture on micro-part based on 2D image as input data of the desired patterns. The 2D image data undergo three processing-step. First is the image preparation and enhancement which includes converting original image into grayscale image. Second step is the XY pre-scaled mapping. The last step is the Z pre-scaled mapping. In this step, the grayscale image color intensity is converted into specified contour height data of micro-texture. Once a complete 3D contour data of micro-texture is obtained, the machining strategy and parameters are determined, and tool paths are then generated. The tool path generation embeds the gouging avoidance scheme throughout the process to produce gouge-free Cutter Location (CL) points. Three 2D input images were used to test the method and algorithm using 3-axis micromilling process on a 5-axis micro-milling machine. The results show that the developed method can successfully produce 3D micro-texture, thus, can be further used for micro-texture surface machining.

Keywords : micro-texturing, micromilling, micro-texture, 2D image processing, gouging avoidance

Introduction

Nowadays, micro scale product has become the needs in various fields such as health, energy, manufacturing, even defense and military application. The micro product could be produced by Micro-Electrical-Mechanical System (MEMS) manufacturing technique, such as photolithography, chemical etching, plating, LIGA, laser ablation, etc. Another method to produce micro product is non-MEMS manufacturing technique (such as EDM, micro-mechanical cutting, laser cutting/patterning/drilling, micro-embossing, micro-injection molding, micro-extrusion, micro-stamping, etc.) [1].

Micro-texture surface is one of the micro scale products, which are used in many applications especially to evoke friction [2-6], to control wettability [7, 8], to alleviate slip [9], lubrication [10, 11], fluid's flow [12], product's art, etc.

The most common process to produce micro-texturing is MEMS manufacturing technique such as etching, laser and lithography, etc. Mata et al. [13] used microfabrication and soft lithography to develop 3D scaffolds with precise micro-architecture and surface micro-texture. The pattern were put on different size thickness layers of SU-8 2100 as the micro-texture patterns. On the other hand, Ziki et al. [14] used spark assisted chemical engraving (SACE) technology to produced micro-texture. Path planning algorithms were used to manufacture straight line channels of the texture pattern. Zhang & Meng [15] utilized

Photochemical machining (PCM), combination of photolithography and wet chemical etching to produce micro-texturing on carbon steel surfaces. The texture pattern was produced by a schematic diagram onpatterned film as film-pasted photomask.

However, research on micro-texture using non-MEMS manufacturing technique is still rare. Kobayashi and Shirai [16] presented a method to generate micro-texture tool path for multi-axis milling machine, one of non-MEMS manufacturing technique. The research used Computer Graphics to make surface texture in micro-product. The texture image pattern was designed using CAD system. An algorithm based on topological features was applied for shape classification. This process was used to classify the shapes of texture pattern. Then, the texture data were converted into STL format, which describes a triangulated surface and was supported by several 3D CAD/CAM applications. Next, the critical points, peaks, pits, and saddle points were calculated from the connection data and STL surface data. CL data were calculated for hills that had similar shapes. The research assumed that the results of machining using this method are better than those using CAM method.

However, from the above conducted researches, it is difficult find the one that handles the micro-texturing based on 2D image.

This paper presents research on non-MEMS manufacturing technique to produce 3D micro-texture based on 2D image processing and carried out by a micro-milling operation. Micro-milling is a micro-scaled conventional milling. The down-scale is effecting the overall cutting parameters such as cutting speed, depth of cut, feed-rate, vibration, thermal effect, etc. In micro-milling, the cutting tools diameter is ranging between 600 µm until 100µm. Due to the micro-size of the tool, the depth of cut is in size of micro and the cutting process needs a high speed spindle rotation which is common between 25.000 rpm to 100.000 rpm. The developed method can be used to easily map the image data, regardless its resolution, into the desired 3D micro-texture data.

The surface texture pattern is generated based on 2D images (a sketch, a picture, a photo or a drawing). This method will simplify the design process of micro-texture pattern. The micro-texture pattern can be directly taken from an artist's sketch, photo, picture or other sources of images with colour degradation. The design perfomance is analyzed by producing actual micro-texture part with the experimental machining process using 3-axis micro-milling. The products of micro-milling process are expected to be matched with the input image texture.

Concept of Micro-Texturing Based on Image Processing

The concept of micro-texturing based on image processing is performed by distinguishing colour intensity or the colour brigh,jtness of an image in order to develop micro-texture pattern and topography. Higher texture area has a brighter colour in-comparison with the lower texture area. Different brightness represents different Z-level. The concept of this method is shown in Fig.1 below.

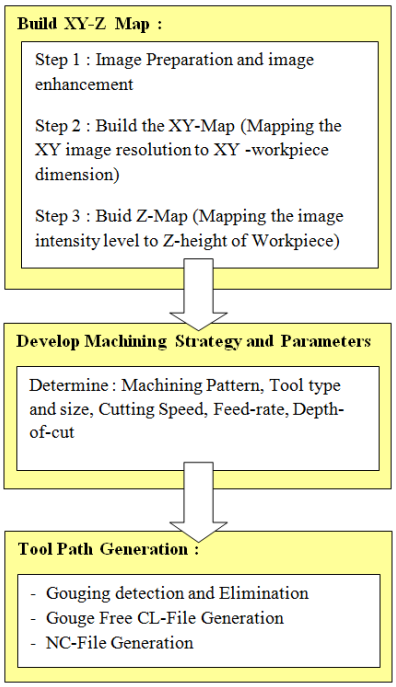

Fig. 1. Concept of Micro-texturing based on 2D Image Processing.

Build The XY-Z Map from Image. Figure 2 shows the image (garter stitch pattern image) used as one of the models in this research, since its pattern represents surface texture. The image can be classified as an artist made image.

Image intensity level is used as a basis for developing 3D contour (topology) information of the micro-texture. This contour information is then used for determining micromilling motion accuracy. The resolution of contour information should not exceed motion resolution of micromilling machine. Therefore the image resizing is conducted, which is effecting the intensity level, to take into account the motion resolution of the micromilling machine.

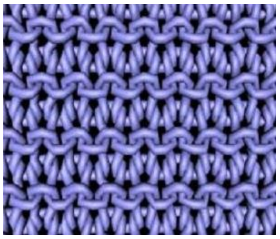

Fig. 2. Original image (garter stitch pattern)

The original image of M x N resolution is then resized to be *m* x *n* resolution which is in this case 254 x 300 pixels. This means the image data array has 254 columns and 300 rows which are along X-axis and Y-axis respectively. Each rows and columns has its own colour intensity value. Intensity of original image is saved in RGB format, which consists of three colour layers. In order to obtain one layer value of intensity, it is needed to convert the original image to become grayscale image as shown in Figure 3. The layer value will be converted into Z-level map. Darker colour represent a lower area of the surface texture while brighter colour represent a higher area of the surface texture. The Z-level will yield the surface pattern that will be machined.

The following rule is used to calculate the XY and Z-value by mapping image intensity value to the designed workpiece topography information.

$$X,Y = \frac{X_W}{X_{res}} \times i, \frac{Y_W}{Y_{res}} \times j \qquad (1)$$

$$Z = Z_w \times \left(1 - \frac{(G_{i,j} - G_{min})}{(G_{max} - G_{min})}\right) \qquad (2)$$

where :

X,Y = X, Y coordinate with respect to the image pixel (i,j) resolution in mm

X_W = specified width of texture on the workpiece in mm

Y_W = specified length of texture on the workpiece in mm

X_{res} = Number of pixel (resolution) along i (X -direction)

Y_{res} = Number of pixel (resolution) along j (Y -direction)

i, j = *i-th* and *j-th* pixel along x and y direction respectively

Z = height of texture on the workpiece at image pixel coordinate (i,j) in mm

Z_W = designed maximum height of texture on the workpiece from the lowest position

$G_{i,j}$ = brightness value of texture at image pixel coordinate (i, j)

G_{min} = minimum brightness value of the image

G_{max} = maximum brightness value of the image

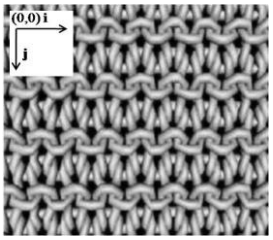

Fig. 3. Grayscale image (garter stitch pattern)

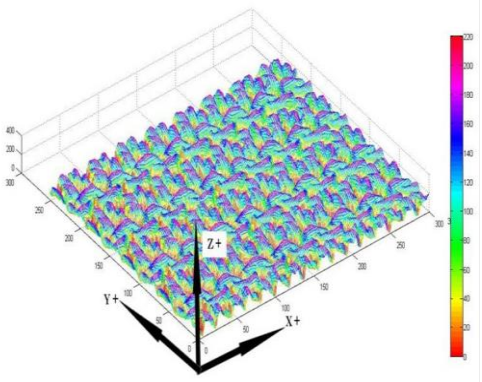

Fig. 4. Z-level mapping conversion (contour view)

The result of mapping from intensity level (intensity domain) of the source image into XY-Z map data (Cartesian domain) is shown in Fig. 4.

After the XY-Z map is obtained, the next step is determining the machining strategy and parameters. Machining parameters are decided with respect to the tool type and size, and tool and workpiece material. The tool path generation is then carried out once the parameters are decided.

Machining Pattern Strategy. Machining pattern is a model of tool movement during cutting operation. There are several machining strategy commonly used in milling operation, such as Parallel Cutting (e.g. Zig, Zig-Zag), Spiral Cutting, Radial Cutting, Follow Part, Follow Periphery, Profile, Zig with Contour, etc. Zig movement is selected in this research (See Figure 5). It aims to produce uniform surface quality since it cuts with the same cutting direction and is easier to manage as well.

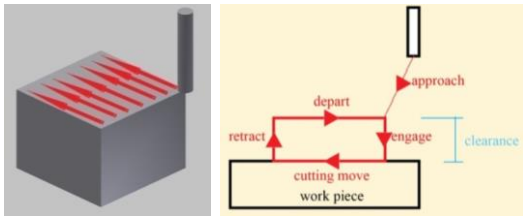

a) b)

Fig. 5. (a) Zig movement (b) Non-cutting movement

Aside the cutting movement, non-cutting movement for the machining process must also be defined. Non-cutting movement includes non-cutting approach, engage, retract and depart. Clearance between initial cutting tool position and workpiece before cutting process begins is set to 0.5mm.

Machining Parameters. The machining parameters and depth of cut arrangement depends on mechanical properties of cutting tools material and workpiece material. Workpiece or specimen material is aluminum (AA7075), while the tools material is Solid Carbide (Seco MEGA-T).

To produce a fine surface with effective time, the machining process is performed in two types of processes : rough milling (roughing) and finish milling (finishing). The roughing process is to remove unintended material as fast as possible, while the finishing one is done to obtain the specified quality of the final machined surface.

Appropriate depth of cut is defined by calculating the tools parameters from tools manufacturer recommendation, as shown in Table 1 and 2.

Table 1. Depth of cut for roughing process [17]

SMG	Coolant	A_p x D_c	A_p x D_c	V_c (m/min)		Milling Roughing D_c (mm)			
						0,1	0,15	0,2	0,3
16	E/M/A	0,75	0,10	500 (450-550)	n (rev/min)	1591550	1061030	795770	530520
					f_z (mm)	0,002	0,003	0,004	0,006
					V_f (mm/min)	6356	6356	6356	6356
17	E/M/A	0,75	0,10	500 (450-550)	n (rev/min)	1591550	1061030	795770	530520
					f_z (mm)	0,002	0,003	0,004	0,006
					V_f (mm/min)	6356	6356	6356	6356

Based on the table 1, with the spindle speed *N* of 75.000 rpm the following machining parameters for roughing process are chosen :

Feed-rate = 1 mm/s
A_p (Dept of Cut - Axial) = 0.06 mm
A_e (Width of Cut - Radial) = 0.02 mm

Since the total depth of workpiece material to be removed in the roughing stage is 0.24 mm, therefore, the roughing process is divided into 4 steps of machining layers : 3 layers with 0.06 mm depth of cut for each layer and 1 layer with 0.0536 mm deph of cut. Fig. 6 – 9 simulate different workpiece surface profile for each machining layer.

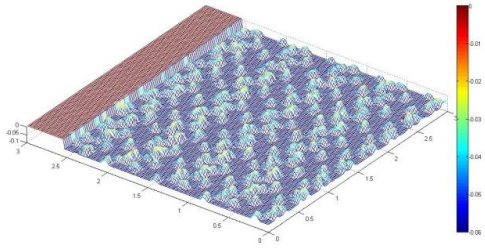

Fig. 6. Graphical simulation of workpiece surface after machining the first layer with depth of cut 0.06 mm

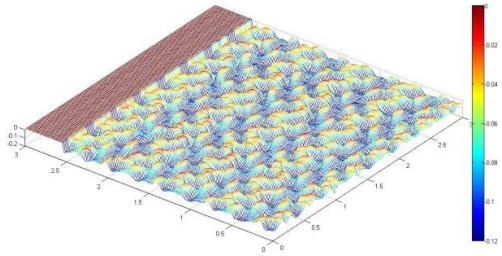

Fig. 7. Simulation of workpiece surface after machining the second layer (reaching 0.12 mm total depth of cut)

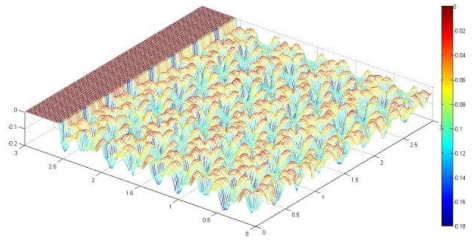

Fig. 8. Simulation of workpiece surface after machining the third layer (with accumulation of depth of cut 0.18 mm)

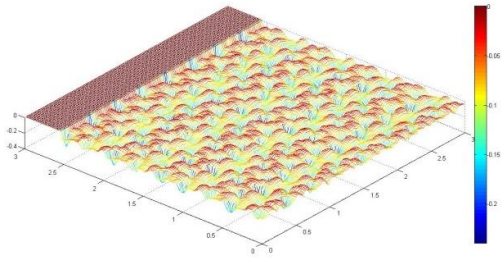

Fig 9. Simulation of workpiece surface after machining the last layer with total accumulation of depth: 0.236 mm

Once the rough milling is completed, the finishing process with spindle speed of 75.000 rpm also is then conducted with the following machining parameters:

Feedrate = 1 mm/s
A_p (Dept of Cut Axial) = 0.004 mm
A_e (Dept of Cut Radial) = 0.02 mm

Table 2. Depth of cut for finishing process [17]

SMG	Coolant	A_p x D_c	A_p x D_c	V_c (m/min)		Milling Finishing D_c (mm)			
						0,1	0,15	0,2	0,3
16	E/M/A	0,04	0,03	600 (550-650)	n (rev/min)	1909860	1273240	954930	636620
					f_z (mm)	0,003	0,005	0,006	0,009
					V_f (mm/min)	11460	11460	11460	11460
17	E/M/A	0,04	0,03	600 (550-650)	n (rev/min)	1909860	1273240	954930	636620
					f_z (mm)	0,003	0,005	0,006	0,009
					V_f (mm/min)	11460	11460	11460	11460

Total depth of cut for finishing the specimen is 0.24 mm as can be seen in Fig.10.

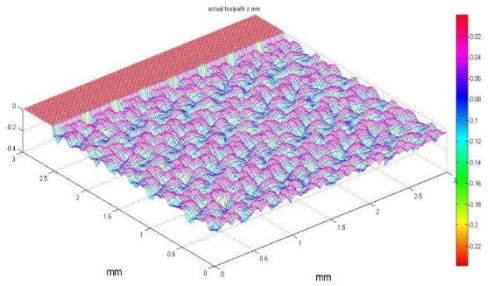

Fig. 10. The surface contour of finishing process after a total depth of cut 0.24 mm

Gouging Avoidance Process. After the image processing step is completed, the next step is tool path generation. In this step, it is important to consider the possibility of gouging. Gouging is a condition where overcut in workpiece occurs during machining process. It can be avoided by using gouging avoidance method in tool path design. Calculating the cutting tool diameter and machine resolution of movement will yield the best result of gouging avoidance method.

Gouging detection is performed by comparing the interference between cutting tool and triangular facets which are generated from the point of the Z-level map. Gouging avoidance calculation in this research is solved using a method proposed by Hwang [18], that is to avoid gouging with vertices, edges and face of triangular facet. The tool lifting for avoiding gouging with vertices of triangles can be seen in the following formula:

$$z_p = z_r + (R^2 - (x_p - x_r)^2 - (y_p - y_r)^2)^2 \quad (3)$$

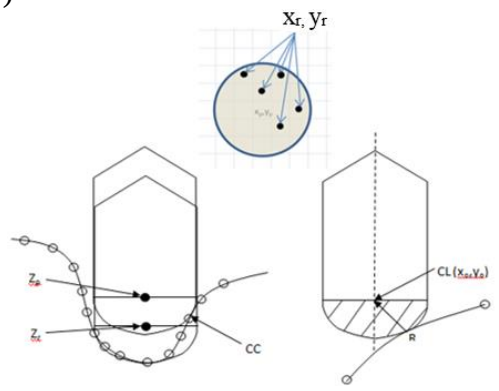

Fig. 11 Scheme of gouging avoidance

Where:

x_p dan y_p = x and y coordinates of cutting tool where the tool is gouge free

x_r, y_r, z_r = vertices coordinates of faceted which are overlapped by cutting tool diameter

R = radius of cutting tool

z_p = z position of cutting tool that is gouge free

When the gouging is detected, the tool is lifted using eq. (3) to barely touch the workpiece surface to have a gouge free tool position (See Figure 11).

At every cc-point, the triangular facets are generated according to all of the Z-level data. Based on triangular facets, the gouging avoidance is carried out. The output of gouging avoidance process is the tool path in CL (Cutter Location) - File format.

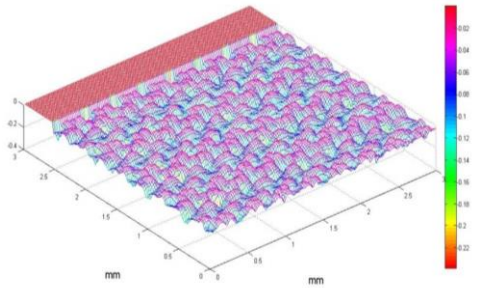

Fig. 12. Simulated surface profile as result of gouging avoidance process

Generate The CL-File and NC-File. After the tool path is successfully generated, the next step is to generate the CL-File. CL-File is a set of sequence of cutting tool position coordinate with respect to the WCS (Workpiece Coordinate System).

The CL-File with ASCII format as a result of tool path generation must be converted using specific postprocessor to the 'NC'-file format with respect to the Machine Coordinate System (MCS) of the micromilling machine. The conversion

between these two coordinate systems are done using inverse kinematic solution which is placed in the postprocessor (Fig. 13).

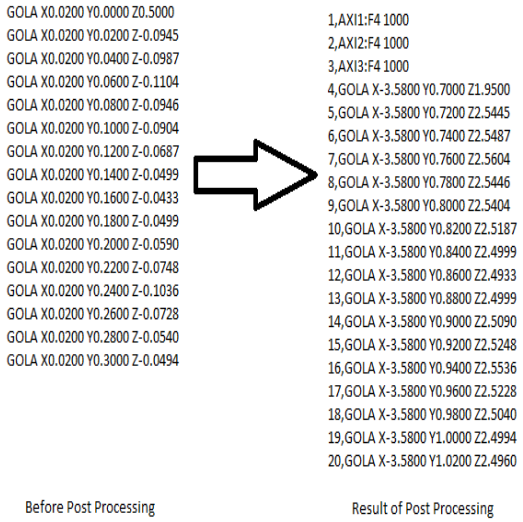

Fig. 13. NC-File conversion

Experimental Setup

Micro-milling machines, like any majority of micro-machine tools, are based on conventional ultra-precision machines that have high accuracy, micro resolution, high rigidity and a temperature-controlled environment. Micro-milling machine consists of a spindle, stages, frames, motors to move each axis of the machine tool and a control system. It is specified to meet the functional requirements of machining operations, like travel, minimum resolution, velocity, accuracy and load capacity.

Micromilling machine used in this experiment is a 5-axis milling machine which consists of 3 motorized linear stage (Suruga Seiki KYC06020-G for XY axis and KS302-30 for Z axis) and two motorized rotary stage (Suruga Seiki KS402-75 and KRW06360). However, in this microtexturing research only 3 axis linear movement are used. The cutting tool is motorized by a high speed air turbine spindle (NSK HTS1501S-M2040) with maximum 150.000 rpm. However, spindle speed (rotation) is set to 75.000 rpm and is measured using a laser digital tachometer (Monarch ACT-3X). Three stepping motor controller (Suruga Seiki DS102 stepping motor controller) is used to regulate the movement of 3 linear stage. The micromilling machine is positioned on the surface of the anti-vibration table to prevent any vibration interference during machining.

The micro-tools used in this experiment is Seco Jabro Mini JM915 solid carbide end mill – ball nose. The carbide end mills – ball nose were coated with MEGA-T (MEGA-T is a proprietary coating exclusive to Seco Tools, Inc). Workpiece material used for this research is aluminum AA7075 with 3x3x3 mm dimension. The tool overhang length from the collet remained constant because the specimens used only one type of cutting tool with 100 µm diameter.

A high-resolution handheld digital microscope (zoom 35x~200x) with resolution up to 1280x1024 is used to monitor the cutting tool movement. The schematic of the micromilling machine set-up and the microtexturing process are shown in Fig. 14 and 15.

NC-file with "prg" file extension format as the result of postprocessor is written in to the micromilling controller. Micromilling machine controller then run the axis stage according to tool position coordinates that have been planned based on 2D image.

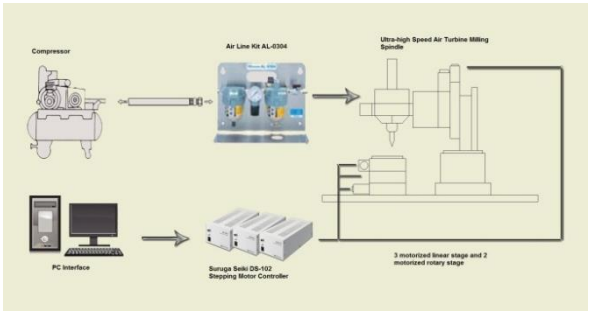

Fig. 14 Schematics of micromilling machine

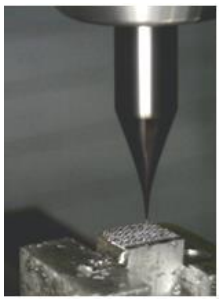

Fig. 15. Microtexturing process

Result and Discussion.

Tool Path and Gouging Avoidance Analysis. Tool path analysis is made by comparing2D image with the tool path that constructed by 2D image processing and with the workpiece as result of machining operation.

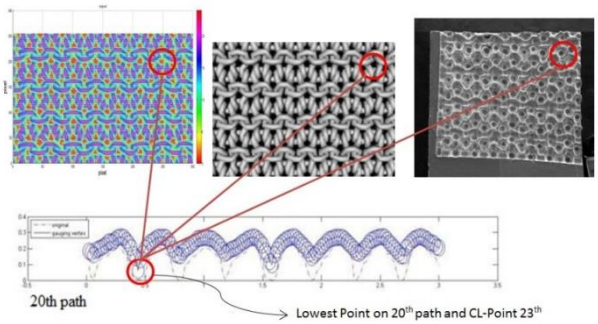

Fig. 16. The valley on the workpiece compared to 2D image

As shown in Fig. 16, at 23th CL-Point of the 20th tool path, there is a spot valley that is generated with respect to color intensity values of the corresponding 2D image. Compared to the surrounding areas, darker area of 2D image forms lower elevation of the tool path.

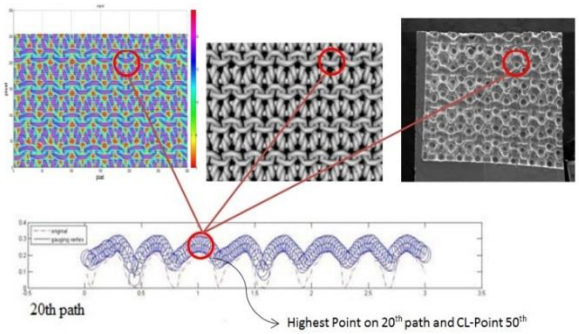

Fig. 17. Cusp of a hill compared to 2D image

On the other hand, on 50th CL-Point of the 20th tool path (as seen in Fig. 17), a hill like contour is formed following color intensity of the corresponding location of the 2D image. The corresponding location on the image shows brighter area (~ higher intensity value) compared to the surrounding ones, therefore a higher tool path elevation is generated on CL-point of that location.

The effectiveness of gouging avoidance scheme is then analyzed. As shown in Fig. 18, the outer tool end surface along path 50th is deviated from the original surface contour. The gouging avoidance process lifted the tool to eliminate detected interference between tool and surface model along the path.

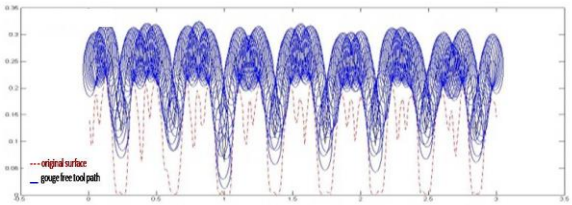

Fig. 18. Tool path 50th compared to the original surface

Furthermore, Fig. 19 shows a comparison among tool path profiles: path 10th, 15th, 20th, and 25th. The profiles, which are different to each others, are influenced not only by the shape of the surface contour along each path but also by the gouging avoidance process at the corresponding path. For example, on the path 15th, it is clearly shown that the tool path is closed to

be linear compared to others. It occurs since the gouging avoidance scheme prevents the tool to go through the narrow valley area which is smaller than the tool diameter.

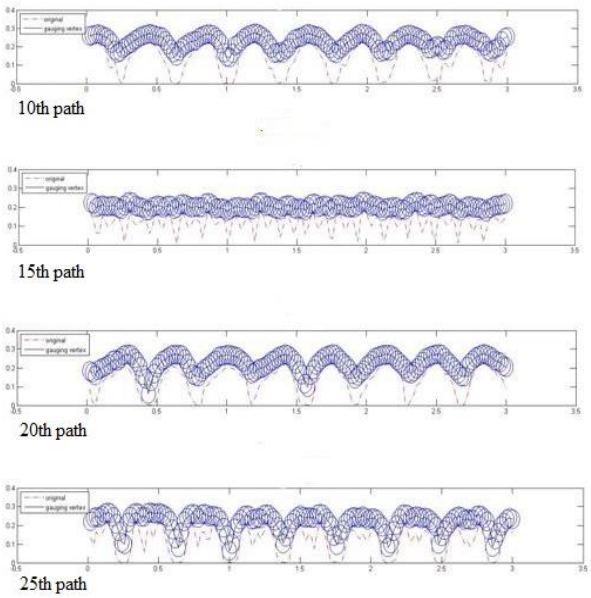

Fig. 19. Comparison among tool path profiles

As the consequence, it can be seen that the final contour (texture) of the machined surface of micro-part, in some area, is quite different compared to the XY-Z map texture as shown in Fig. 4 and 5.

In more detailed, effectiveness of gouging avoidance can be more seen in Fig. 20 and 21. Fig. 20 explains that three consecutive tool paths 50th, 51st, and 52nd have relatively the same path profile since they passed relatively the same surface contour.

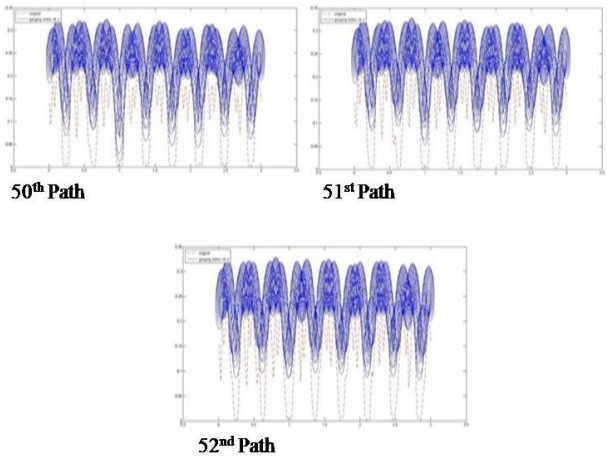

Fig. 20 Consecutive tool paths (50th, 51st, and 52nd) with relatively the same path profile

Moreover, as shown in Fig. 21, at the same location (blacked circle) of 90th and 95th path along X-axis and 20th path along Y-axis, the tool could not go down to lower position even though the contour is seemed feasible. It occurs since there exists other neighboring contour has narrower gap that could be interfered when the tool goes down. This contour is actually located at more or less the same location of 100th path in Fig. 21.

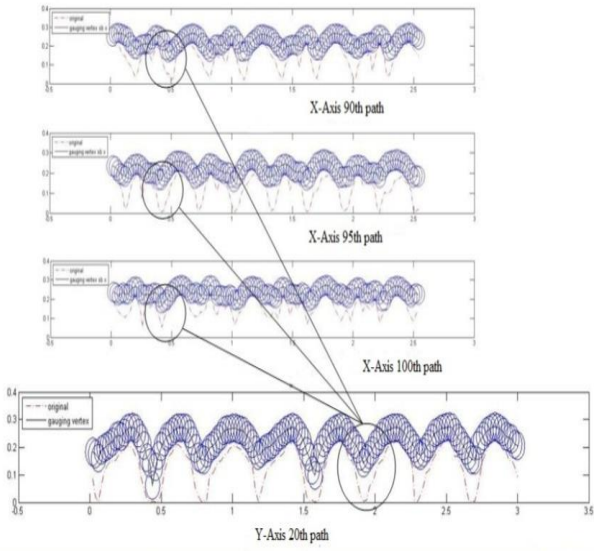

Fig. 21. Tool paths influenced by neighboring contour

When the tool is changed with different diameters, it is clearly shown (Fig. 22) that the tool path is going along with the tool diameter in the sense that the tool size (diameter) influences the gouging avoidance scheme to react accordingly to avoid the tool interferes the surface.

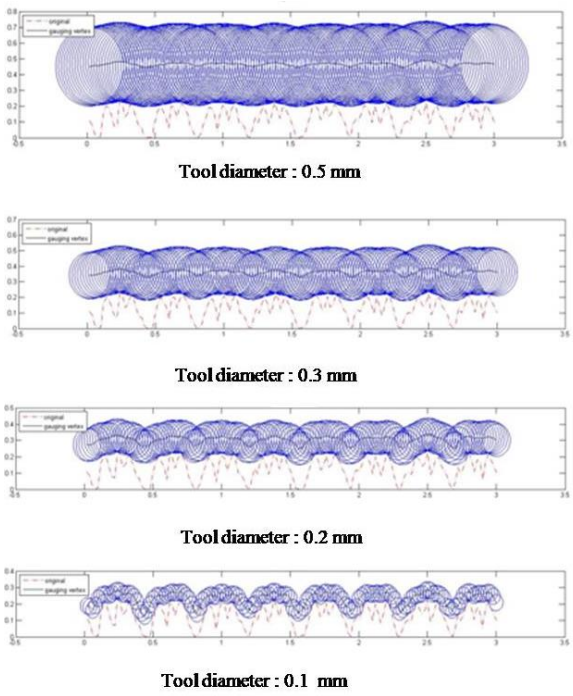

Fig. 22 Tool path profiles with different tool diameters on the same surface contour

Machining Result Analysis. Fig. 23 shows the final workpiece of microtexturing that is compared with a match.

Fig. 23. Result of microtexturing compared to actual product (a match)

Scanning Electron Microscope (SEM) is used to get a clearer image and to see the structure of workpiece as result of microtexturing operation for further analysis. Black dots that are shown in Fig. 24 (a) and 25 (a) represent deeper surface contour compared to the neighboring surface area.

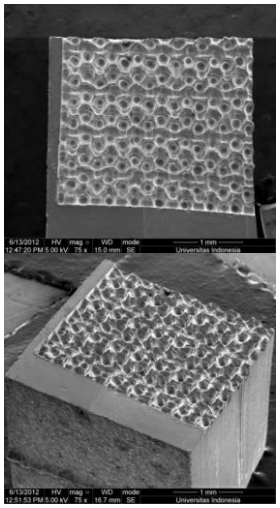

a) b)

Fig. 24 (a) Top view and (b) Isometric view of machining result image with resolution of 127 x 150 pixels

The valleys and hills are formed as expected by using the developed image processing method.

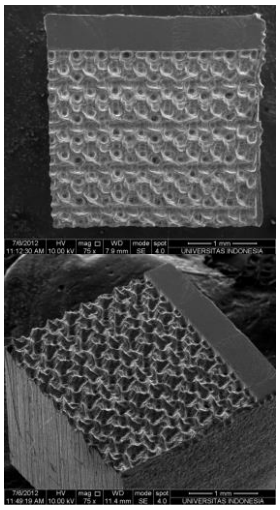

a) b)

Fig. 25 (a) Top view and (b) Isometric view of machining result image with resolution of 254 x 300 pixels

Two image resolutions are tested : 254 x 300 and 127 x 150. It is shown that image resolution setting influences the machining result. Image with 254 x 300 pixel produces smoother and more detailed texture as shown in Fig. 29 and Fig. 30, compared to image with 150 x 127 pixel resolution. The higher image resolution that mapped to the same area of workpiece, the more CC-point generated in each tool path.

As previously mentioned in gouging analysis section, there are differences between surface texture directly generated from the image (Fig. 4) and the actual micro-texture of the machined surface (Fig. 24 and Fig. 25). This difference occurs due to final cutting path is modified by gouging avoidance scheme. When the gouging is detected, e.g. when the tool diameter is bigger than the surface contour of the texture (See Fig. 22), the gouging avoidance scheme calculates the non-gouge free CL-point. Therefore, eventually the cutting path profile changes the surface texture accordingly to avoid overcut.

In order to have more tests on the method with different surface texture, other two different 2D images with 254 x 300 pixel resolution are used, as shown in Fig. 33 and 35. The cutting tool diameter is 0.1mm for finishing operation and other cutting parameters are set to be the same with the previous microtexturing. The gray scale image and microtexturing results are shown in Fig. 26 and 27.

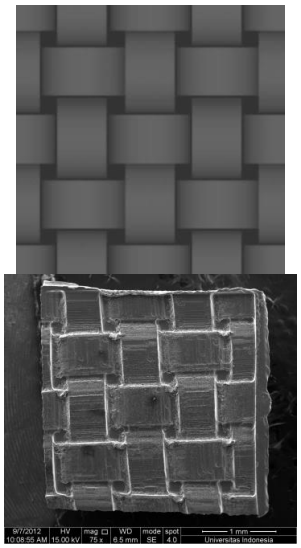

a) b)

Fig. 26 (a) Grayscale image as the source of (b) micro-texturing result

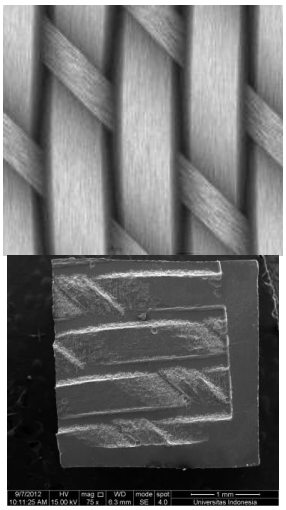

Fig. 27 (a) Grayscale image as the input image of (b) micro-texturing result

The image patterns can be fully developed using tool diameter 0.1mm with minimum tool lifting compared to the initial pattern (garter stitch). Therefore, the machining results show that the corresponding 2D images can be generated successfully on the workpieces.

Conclusion

The developed method is proven to be a simple method to generate micro-texture pattern based on 2D image processing. A

2D image of texture such as hand sketch, picture or photograph that has colour degradation or brightness differences with respect to its contour height can be directly used to generate tool path for 3-axis micromilling operation through image processing.

The total depth of micro-texture (contour), the distance between the highest point on the texture surface to the lowest one, can be determined suitably. Furthermore, the texture area represented by image resolution can be mapped onto any dimension (*length* x *width*) of the workpiece (micro-part) flexibly. An image can be simply arranged to be an array of the same image to produce a micro-texture with wider area.

Image with higher resolution would produce a more detailed micro-texture as long as within the machining motion resolution and the tool diameter that is used can protrude to the vicinity of the micro-texture contour without gouging.

ACKNOWLEDGEMENT

This research was funded by Research Grant 2012 from Universitas Indonesia and Yeungnam University – Korea.

REFERENCES

[1] Yi Qin, Book Chapter of 'Micro-manufacturing Engineering and Technology, Elsevier, 2010.

[2] G. Ryk, Y. Kligerman, I. Etsion, 'Experimental invetigation of laser surface texturing for reciporating automotive components', Tribology Trans. 45 (2002) 444–449.

[3] Z. Schuss, I. Etsion, 'On the solution of lubrication problems involving narrow configurations', ASLE Trans. 24 (1981) 186–190.

[4] Q. J. Wang, D. Zhu, R. Zhou, F. Hashimoto, 'Investigating the effect of surface finish on mixed EHL in rolling and rolling-sliding contacts', Tribology Trans. 51 (2008) 748–761.

[5] B. He, W. Chen, Q.J. Wang, Surface texture effect on friction of a micro-textured poly (dimethylsiloxane) (PDMS), Tribology Lett. 31 (2008) 187–197.

[6] David Salamon, Rob G.H. Lammertink, Matthias Wessling, Surface texturing inside ceramic macro/micro channels, Journal of the European Ceramic Society 30 (2010) 1345–1350.

[7] Sommers AD, Jacobi AM., Creating micro-scale surface topology to achieve anisotropic wettability on an aluminum surface, Journal of Micromechanicsand Microengineering (2006);16:1571–8.

[8] Kim TI, Dongha T, Hong HL., Wettability-controllable super water- and moderately oil-repellent surface fabricated by wet chemical etching, Langmuir (2009);25:6576–9.

[9] Moronuki, Nobuyuki, Kaneko, Arata, Safe and comfort design of micro-structured surface for artifacts in contact with human, Key Engineering Material (2010) 447-448 : 690 – 694.

[10] Q.J. Wang, D. Zhu, Virtual texturing: modeling the performance of lubricated contacts of engineered surfaces, Journal of Tribology 127 (2005) 722–728.

[11] T. Nanbu, N. Ren, Y. Yasuda, D. Zhu, Q.J. Wang, Micro textures in concentrated conformal-contact lubrication effects of texture bottom shape and surface relative motion, Tribology Lett. 29 (2008) 241–252.

[12] Taylor JB, Carrano AL, Kandlikar SG., Characterization of the effect of surface roughness and texture on fluid flow—past, present, and future, International Journal of Thermal Sciences (2006);45:962–8.

[13] Alvaro Mata,Eun Jung Kim, Cynthia A. Boehm, Aaron J. Fleischman, George F. Muschler, Shuvo Roy, A three-dimensional scaffold with precise micro-architecture and surfacemicro-textures, Biomaterials 30 (2009) 4610–4617.

[14] Jana D. Abou Ziki, Tohid Fatanat Didar, Rolf Wüthrich, Micro-texturing channel surface sun glass with spark assisted chemical engraving, International

Journal of Machine Tools & Manufacture 57 (2012) 66–72
[15] Jinyu Zhang &Yonggang Meng, A study of surface texturing of carbon steel by photochemical machining, Journal of Materials Processing Technology 212 (2012) 2133– 2140.
[16] Kobayashi Y., Shirai K., , Multi-axis Milling for Micro-texturing, International Journal of Precision Engineering and Manufacturing, Vol. 9, No.1, pp 34-38, 2008
[17] SECO-JABRO, Catalog of Micro-milling Cutting Tools, 2012.
[18] Hwang, J.S., Interference-free tool-path generation in the NC machining of parametric compound surfaces, Computer Aided Design, 24 : 667-676, 1992